The mechanism of light gas transport through configurational free volume in glassy polymers

William J. Box[1], Zihan Huang[2], Ruilan Guo[2] and Michele Galizia[1]*

[1] *School of Chemical, Biological and Materials Engineering, University of Oklahoma, 100 E. Boyd Street, Norman 73019, OK, USA*

[2] *Department of Chemical and Biomolecular Engineering, University of Notre Dame, 205 McCourtney Hall, Notre Dame 46556, IN, USA*

Submission to the Journal of Membrane Science, **REVISED MANUSCRIPT**

*Corresponding Author: Prof. Michele Galizia, *mgalizia@ou.edu*

Graphical Abstract

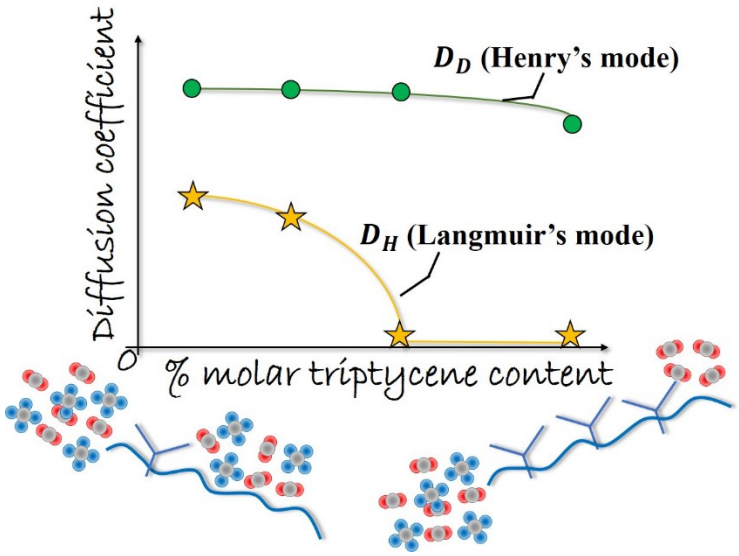

Abstract

A possible mechanism of small molecule transport in glassy polymer membranes containing configurational free volume (i.e., triptycene moieties) is proposed. To this aim, a family of triptycene-containing polybenzoxazoles (TPBOs) exhibiting systematically varied molar amount of triptycene units, ranging from 25% to 100%, was selected to perform a light gas (N_2, CH_4 and CO_2) fundamental sorption-transport study. The dual mode sorption-mobility model was used to isolate the effect of configurational free volume on penetrant transport. CO_2 and CH_4 Henry's and Langmuir's mode diffusion coefficients were estimated and used to quantify the Henry's and Langmuir's contributions to CO_2/CH_4 diffusivity-selectivity as a function of the triptycene molar content in TPBOs. Interestingly, while the Henry's CO_2/CH_4 diffusivity-selectivity changes little with increasing amount of configurational free volume, the Langmuir's CO_2/CH_4 diffusivity-selectivity increases up to infinity when the molar triptycene concentration in the polymer is 75% or higher, showing that the diffusion of larger molecules (i.e., CH_4) is increasingly hindered relative to smaller molecules (i.e. CO_2) diffusion when more configurational free volume is incorporated in the polymer. In sharp contrast, pure- and mixed-gas sorption, as well as solubility-selectivity, is essentially unaffected by the triptycene molar content. According with this physical picture, the analysis of isosteric heats of CO_2 sorption indicates that TPBOs plasticization resistance is independent of triptycene content.

Keywords: configurational free volume; triptycene; Henry's diffusivity-selectivity; Langmuir's diffusivity-selectivity; solubility-selectivity

1. Introduction

Since 1991, the introduction of advanced polymer synthesis strategies allowed membrane separations to become competitive with traditional thermal-based separation technologies. A plethora of novel functional polymers, purposely designed to achieve specific molecular separations, were synthesized with the scope of addressing three major issues: the selectivity/permeability trade-off, physical aging and plasticization [1-15].

Although it was originally reported solely for gas separation membranes, the existence of a selectivity/permeability trade-off has also recently been observed in liquid separation membranes, including water purification and organic solvents separation [16-19]. For this reason, most of research in the field has focused on the discovery and development of advanced membrane materials that can surpass the upper bound while achieving an economically attractive performance. As a consequence, most of the gas separation upper bounds first reported by Robeson in 1991 [3], were updated in 2008 [4] taking in consideration new materials appeared in the market in the previous seventeen years: perfluoropolymers, which were the subject of intense research in the late '90s, were essentially responsible for this improvement [4, 20]. In 2019, the discovery of a new class of polymers of intrinsic microporosity (PIMs) bearing benzotriptycene moieties allowed to further push up and re-define the upper bound in several gas separation applications [21].

Since the pioneering study reported by Park in 2011 [22], glassy polymers containing triptycene units and their derivatives emerged as an interesting platform of materials [5, 8, 23-26]. Triptycene groups, made of three benzene rings arranged in a 3D paddlewheel-like configuration, provide their unique configurational free volume, which promotes high permeability while maintaining

it stable over long-term operation [5, 23, 27, 28]. Moreover, while the size of excess conformational free volume pockets in conventional glassy polymers is randomly distributed [29], the size of configurational free volume elements is highly uniform and it is comparable to the size of a single molecule, which promotes high selectivity [5, 30, 31]. Thermally-rearranged polybenzoxazoles containing triptycene units, reported by Guo et al. [25], outperform the 2008 upper bound in several gas separations involving hydrogen and carbon dioxide, and maintain their performance unchanged even after a harsh thermal pre-treatment [32].

Most of the newly reported membrane materials are glassy, due to their higher selectivity compared to rubbery polymers. However, conformational free volume available for small molecule transport in conventional glassy polymers, which comes from frustrated chain packing, makes these materials susceptible to physical aging [1, 2, 8, 33-36]. The latter issue, i.e., the non-equilibrium excess free volume relaxation, represents an important limitation for using glassy polymers in membrane applications [8, 34]. Triptycene-based polymers may offer an attractive solution to this issue. Unlike the conformational free volume provided by conventional glassy polymers, which originates from inefficient chain packing, the internal free volume provided by the triptycene units is related to the molecular configuration and, as such, it is non collapsible, similar to inorganic (e.g., zeolites) or hybrid (e.g., MOFs) materials [5, 8, 23, 26, 31, 32]. As shown in recent studies [23, 24, 26, 32], glassy polymers exhibiting configurational free volume (i.e., triptycene and pentiptycene groups) exhibit reduced physical aging propensity compared to conventional glassy polymers exhibiting only conformational free volume.

Although preliminary studies reported a reduced hysteresis upon subsequent sorption-desorption CO_2 cycles at high pressure in triptycene-based polymers [37, 38], additional research efforts are needed to investigate in detail the plasticization propensity of these materials.

For all of the reasons listed above, iptycene-based materials are garnering increasing attention in membrane science. However, despite the current progress, fundamental understanding of small molecule transport in glassy polymers exhibiting configurational free volume is still poor and incomplete. Only recently, Box et al. reported that the transport of bulky vapor molecules in thermally rearranged triptycene-based polybenzoxazoles (TPBOs) is limited by entropic factors, with both sorption and diffusion being controlled by penetrant size [39]. To fill this fundamental knowledge gap, in this study we provide a detailed description of the molecular mechanism of light gas transport in polymers exhibiting configurational free volume. A series of thermally rearranged polybenzoxazoles (TPBOs) exhibiting systematically varied molar amounts of triptycene units was selected as a platform to develop structure-property correlations, with the final goal of understanding the mechanism by which configurational free volume regulates selectivity in membrane separations.

2. Theoretical background

2.1 Gas sorption and transport in polymers. Gas transport in dense (i.e., non-porous) polymer membranes is described by the solution-diffusion model, according to which the permeability coefficient, $\wp$, is given by the product of the diffusion and sorption coefficients [40]:

$$\wp = \overline{D} \times S \qquad \text{(Eq. 1)}$$

where the apparent solubility coefficient, S, is defined as C/f, C being the penetrant concentration in the upstream membrane face and f the feed penetrant fugacity [1, 2, 40]. $\overline{D}$ is the effective, concentration-averaged penetrant diffusion coefficient [41].

A Van't Hoff-type relationship describes the temperature dependence of gas sorption in polymers [42, 43]:

$$S = S_0 exp\left(-\frac{\Delta H_S}{RT}\right) \qquad \text{(Eq. 2)}$$

where ΔH_S is the enthalpy of sorption and S_0 is a pre-exponential constant. The enthalpy of sorption is given by the sum of the penetrant condensation enthalpy, ΔH_{cond}, and the penetrant/polymer mixing enthalpy, ΔH_{mix}, which takes into account *i)* the polymer-penetrant interactions and *ii)* the deformation work needed to open gaps between polymer chains to accommodate penetrant molecules in the Henry's mode [43, 44].

The analysis of sorption isotherms at multiple temperatures provides the isosteric heat of sorption, that is, the concentration dependence of ΔH_S [42]:

$$\left[\frac{d(lnp)}{d\left(\frac{1}{T}\right)}\right]_C = \frac{\Delta H_S}{ZR} \qquad \text{(Eq. 3)}$$

where p is the pressure corresponding at each concentration (i.e., C) at a given temperature T, and Z is the compressibility factor [42].

The membrane ideal (i.e., pure-gas) selectivity, which is defined as the ratio of pure gas permeabilities at the same temperature and pressure, can be expressed as the product of the diffusivity-selectivity, which quantifies the polymer size-sieving ability, and the solubility-selectivity, which quantifies the polymer's ability to separate molecules based on their condensability and thermodynamic affinity with the membrane material [40, 45]:

153 $$\alpha_{ij}^{id} = \frac{\wp_i}{\wp_j} = \frac{\bar{D}_i}{\bar{D}_j} \times \frac{S_i}{S_j} = \alpha_D^{id} \times \alpha_S^{id}$$ (Eq. 4)

154

155 *2.2 Dual Mode Sorption-Transport Model.* The Dual Mode Sorption-Transport model provides a
156 phenomenological, although physically sound quantitative description of small molecule
157 sorption and diffusion in glassy polymers as a function of the pressure and temperature, enabling
158 a direct correlation of the transport properties with the membrane structure [46-49]. According to
159 the dual mode approach, the penetrant concentration in the polymer, C, is given by the sum of
160 concentration in the equilibrium, rubber-like polymer phase (Henry's population) and the
161 concentration in pre-existing free volume pockets (Langmuir's population) [46, 50]:

162 $$C = k_D f + \frac{C_H' b f}{1 + b f}$$ (Eq. 5)

163 where k_D is the Henry's constant, C_H' is the Langmuir sorption capacity, b is the Langmuir affinity
164 parameter and f is the penetrant fugacity in the external gas phase.
165 Using the solution-diffusion model, the dual mode model can be promptly extended to describe
166 not only equilibrium sorption, but also small molecule transport in glassy polymers [50]. This can
167 be done by assigning a non-zero mobility to both the Henry's and the Langmuir's populations,
168 giving rise to the dual sorption-mobility model [46, 50]:

169 $$\wp = k_D D_D \left(1 + \frac{KF}{1 + bf}\right)$$ (Eq. 6)

170 where D_D and D_H are the diffusion coefficients of the Henry's and Langmuir's population,
171 respectively, assumed constant, and F and K are constants defined as $F = D_H/D_D$ and $K =$
172 $C_H' b/k_D$, respectively [50]. All the remaining parameters have the usual physical meaning and are
173 taken from the analysis of single gas sorption data at the same temperature.

When considering the sorption of a mixture of n components in a glassy polymer at a given temperature, the dual mode theory provides the following expression for the concentration of species i in the polymer [51]:

$$C_i = k_{D,i} f_i + \frac{C'_{H,i} b_i f_i}{1+\sum_{i=1}^{n} b_i f_i} \qquad \text{(Eq. 7)}$$

where the fugacity of the *i-th* component, f_i, is a function of pressure and gas mixture composition. Remarkably, the dual mode parameters appearing in Eq. 7 are those retrieved from the analysis of pure gas sorption at the same temperature as the mixture, therefore, absent polymer swelling and specific penetrant-penetrant and penetrant-polymer interactions, the dual mode model can reliably predict mixed gas sorption [51]. According to Eq. 7, competitive sorption into the Langmuir sites, due to the presence of the multiple components, reduces the concentration of species i in the polymer compared to pure species sorption at the same temperature and fugacity [51, 52].

At any given pressure, temperature and mixed-gas composition, the mixed-gas sorption coefficient of species i and the i-to-j real solubility-selectivity are given by Eqs. 8 and 9, respectively [37]:

$$S_i^{mix} = \frac{C_i^{mix}(f_i)}{f_i} \qquad \text{(Eq. 8)}$$

$$\alpha_S^{mix} = \frac{S_i^{mix}}{S_j^{mix}} \qquad \text{(Eq. 9)}$$

3. Experimental

3.1 TPBO synthesis and membrane fabrication. To investigate the effect of configurational free volume on the mechanism of small molecule transport in polymers, co-polyimides containing systematically varied molar amount of triptycene units (25, 50, 75, 100%) were synthesized

according to the protocol described in ref. [25] and briefly summarized in the Supporting Information. Flat, free standing films of the triptycene-containing co-polyimides were thermally rearranged at 300°C for 2h and then at 450°C for 30 min, under nitrogen purge, to form fully converted triptycene-based polybenzoxazoles (TPBOs). The TPBOs structure is shown in Table 1, along with some relevant structural and physical properties.

Table 1. *Structure and physical properties of TPBOs.*

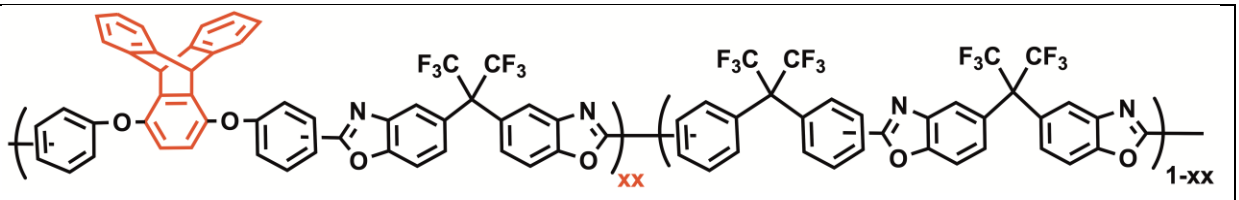

triptycene molar content (xx)	*density* (g/cm³)*	*T_g (°C)*	*FFV§ (%)*	*d-spacing† (Å)*	*%TR conversion‡*
25%	*1.393 ± 0.002*	*> 400*	*22.6*	*6.4*	*100*
50%	*1.369 ± 0.015*	*> 400*	*20.5*	*6.6*	*100*
75%	*1.346 ± 0.016*	*> 400*	*18.9*	*7.0*	*100*
100%	*1.324 ± 0.004*	*> 400*	*17.4*	*7.2*	*100*

** density was determined at room temperature using an Archimede's balance and water as the buoyant fluid. The experimental uncertainty was calculated from the standard deviation of 6-8 independent measurements.*

§ FFV was calculated using the group contribution method [53].

† d-spacing was calculated from WAXD experiments [25].

‡ full (i.e., 100%) thermal conversion to TPBOs was confirmed by FTIR spectroscopy [25].

3.2 Sorption and transport measurements. Pure gas N_2, CH_4 and CO_2 sorption isotherms at multiple temperatures (20, 27, 35 and 50°C for TPBO-0.50, TPBO-0.75, TPBO-1.00; 5, 20, 35 and 50°C for

211 TPBO-0.25) and up to 35 atm were measured using a dual volume barometric apparatus, whose
212 main features are summarized in Fig. S1, Supporting Information. The Peng-Robinson equation
213 of state was used to solve the molar balances needed to generate the sorption isotherms [54].
214 Pure gas N_2, CH_4 and CO_2 permeability data at 35°C were taken from ref. [25]. Diffusion
215 coefficients at 35°C were calculated via the solution-diffusion model [40], using experimental
216 solubility and permeability data.
217

218 **4. Results and Discussion**

219 *4.1. Pure-gas sorption as a function of temperature and triptycene molar content*. Pure-gas CO_2 sorption
220 isotherms at 35°C in TPBOs exhibiting systematically varied molar amount of triptycene units
221 (i.e., 25, 50, 75, 100%) are shown in Fig. 1A, in the units of cm^3(STP)/cm^3(polymer), as a function
222 of CO_2 fugacity. Experimental uncertainty was estimated using linear error propagation [55],
223 taking into account the uncertainty of *i)* the volumes of the sorption and charge chambers, *ii)* the
224 pressure transducers reading, *iii)* the temperature controller reading and *iv)* the polymer density.
225 Pure gas fugacity was calculated at any temperature and pressure using the Peng-Robinson
226 equation of state (cf. Table S1, Supporting Information) [54].
227 All the isotherms, at all temperatures and for all TPBO samples, exhibit the typical dual mode
228 shape. CO_2 sorption isotherms in TPBOs at 35°C are, within the experimental uncertainty,
229 superimposed over each other (cf. Fig.1A), which indicates that gas solubility in TPBOs is
230 essentially independent of the triptycene content, despite the free volume decreases from 22.6%
231 to 17.4% with increasing the triptycene molar content from 25% to 100% (cf. Table 1). Similar

results were obtained at the other temperatures inspected, 20, 27 and 50°C (cf. Fig. S2, Supporting Information).

Similar to CO_2, CH_4 and N_2 solubility in TPBOs at any temperature is essentially independent of the triptycene molar content. For the sake of brevity, CH_4 and N_2 sorption isotherms in TPBOs at 35°C are shown in Fig. 1B-C, respectively, while isotherms at other temperatures are shown in Fig. S3-S4, Supporting Information.

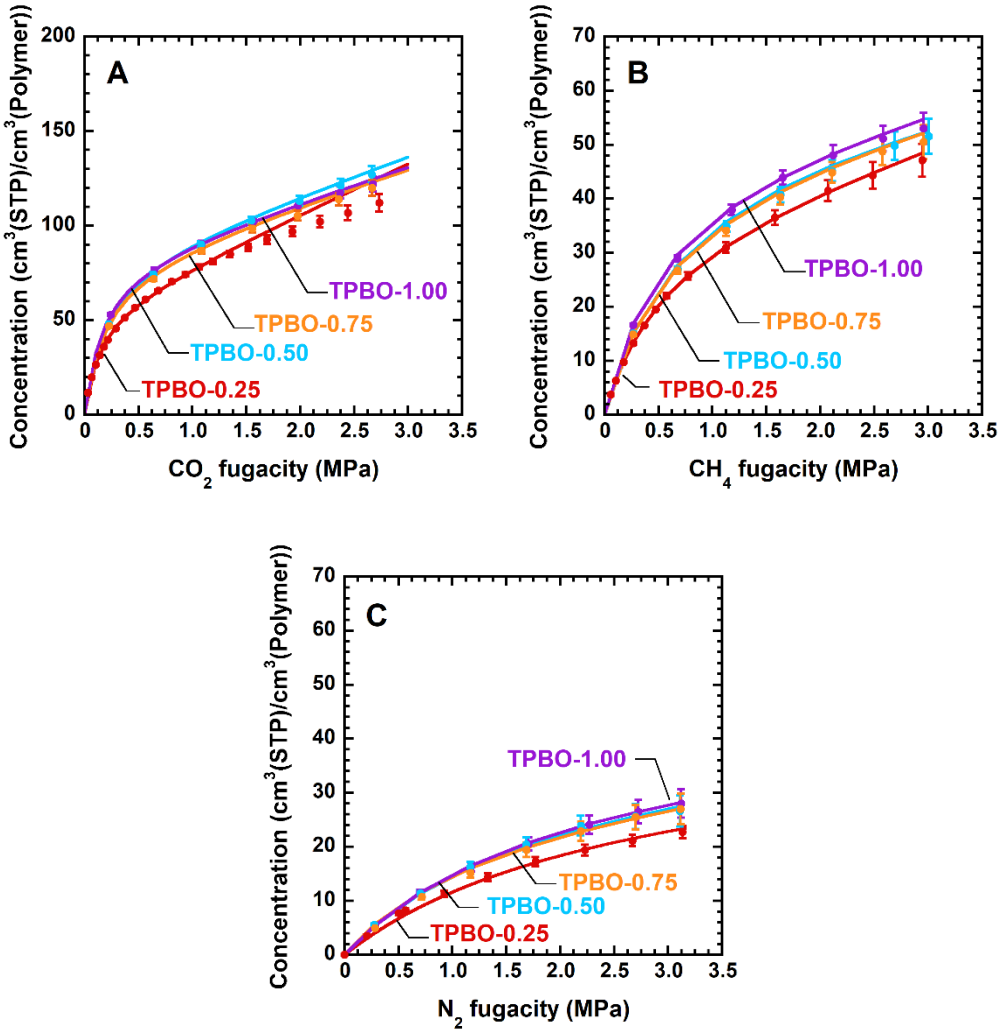

Figure 1. *CO_2 (A), CH_4 (B) and N_2 (C) sorption isotherms at 35°C in TPBO samples exhibiting different molar amount of triptycene units. Continuous lines represent the dual mode fitting. Experimental uncertainty was calculated using linear error propagation [55].*

Sorption isotherms in TPBO-0.25 apparently deviate from those collected for other TPBO samples (i.e., TPBO-0.50, TPBO-0.75, TPBO-1.00). It is worth mentioning that sorption data in TPBO-0.25 were measured in a previous study from this laboratory [37], using samples from a previous synthesis batch, which explains the origin of this slight deviation. However, if we take the experimental uncertainty into account (cf., Figs. 1), these differences turn out to not be significant. CO_2 sorption isotherms at multiple temperatures (20-50°C for TPBO-0.50, TPBO-0.75 and TPBO-1.00, 5-50°C for TPBO-0.25) and given triptycene molar content are shown in Fig. 2. For the sake of brevity, CH_4 and N_2 sorption data in the same temperature range are shown in the Supporting Information (cf. Fig S5 and S6). Consistently with the typical behavior of glassy polymers, at any given external fugacity, gas sorption in TPBOs decreases with increasing temperature [42].

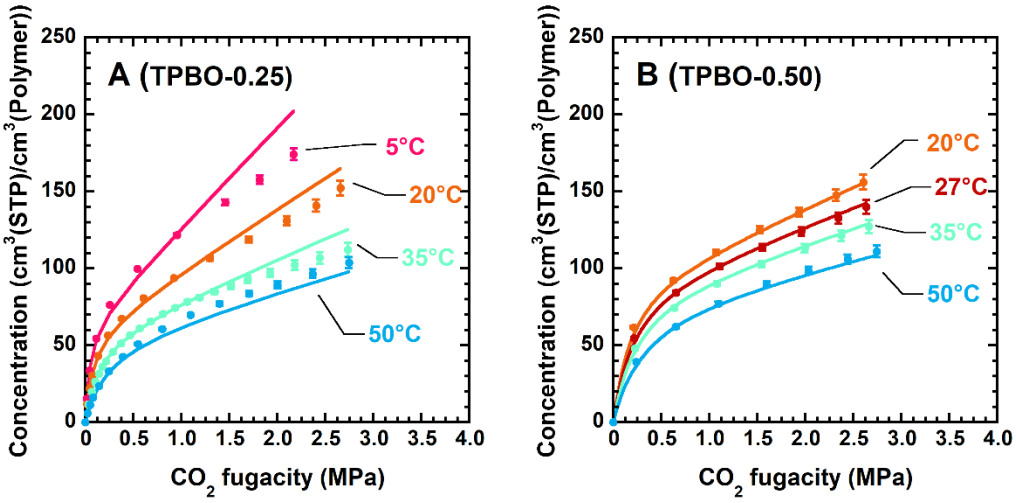

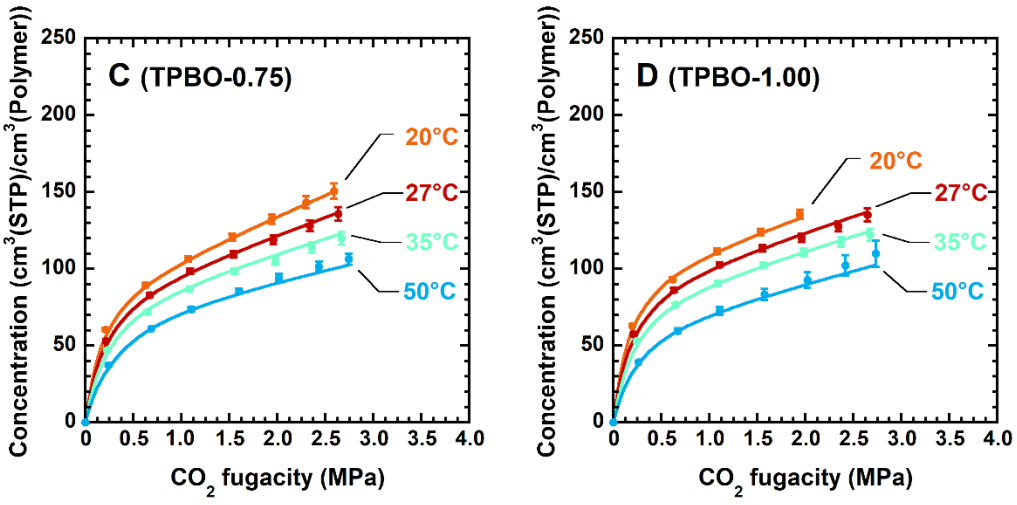

Figure 2. *CO_2 sorption isotherms at multiple temperatures in A) TPBO-0.25, B) TPBO-0.50, C) TPBO-0.75 and D) TPBO-1.00. Solid symbols: experimental data. Continuous lines: dual mode fitting. Experimental uncertainty was calculated using linear error propagation [55].*

As shown in Figs. 1 and 2, the dual mode model was used to correlate the experimental sorption isotherms. Since different sets of dual mode parameters can describe a given set of experimental data [37, 56], the fitting was performed with constraints on K_D, C'_H and b as a function of temperature (cf. Table 2).

Table 2. *Constraints used for the dual mode fitting of sorption data at multiple temperatures in TPBOs.*

dual mode parameter	*constraint*		*introduced parameters*
K_D	$K_D = K_{D_0} \exp\left(-\frac{\Delta H_{K_D}}{RT}\right)$	*Van't Hoff relationship*	K_{D_0}, ΔH_{K_D}
C'_H	$C'_H = C'_{H_0} - mT$	*temperature dependence of* C'_H	C'_{H_0}, m
b	$b = b_0 \exp\left(-\frac{\Delta H_b}{RT}\right)$	*Van't Hoff relationship*	b_0, ΔH_b

Specifically, we assumed: *i)* a Van't Hoff dependence of the Henry's parameter, K_D, on temperature [37, 56]; *ii)* a linear decrease of the Langmuir's sorption capacity, C'_H, with increasing temperature, according to the physical picture that C'_H vanishes when T approaches T_g [57]; *iii)* a Van't Hoff dependence of the Langmuir's affinity parameter, b, on temperature [37, 56]. The six introduced fitting parameters (i.e., $K_{D\,0}$, ΔH_{K_D}, $C'_{H\,0}$, m, b_0 and ΔH_b) provide a good parametrization of the sorption isotherms collected for each TPBO sample at multiple temperatures. No significant difference in fitting accuracy was observed in the constrained fitting compared to that of the individual dual mode fittings. The complete set of dual mode parameters for N_2, CH_4 and CO_2 sorption in TPBOs are shown in Tables S2-S5, Supporting Information, along with the uncertainty analysis, which was carried out through linear error propagation [55]. For the sake of brevity, a general discussion of the results of dual mode modeling is reported in the Supporting Information. For example, consistently with the dual mode analysis of gas sorption in triptycene-free thermally rearranged polymers proposed by Stevens et al. [56], ΔH_{K_D} and ΔH_b are negative, indicating that K_D and b decrease with increasing temperature. Moreover, at any given temperature and in all TPBO samples, the logarithm of K_D increases linearly with penetrant critical temperature (i.e., $ln(K_D) = MT_C + N$) with a slope of 0.015K^{-1}, which is consistent with previous literature reports (cf. Fig. S7, Supporting Information) [37, 56, 58]. Remarkably, the latter feature is captured by the model without imposing any additional constraints, which confirms that the model fitting is self-consistent and physically meaningful.

4.2. Isosteric heats of sorption. The isosteric heat of sorption, that is, the enthalpy of N_2, CH_4 and CO_2 sorption as a function of penetrant concentration in TPBOs, is shown in Figs. 3.

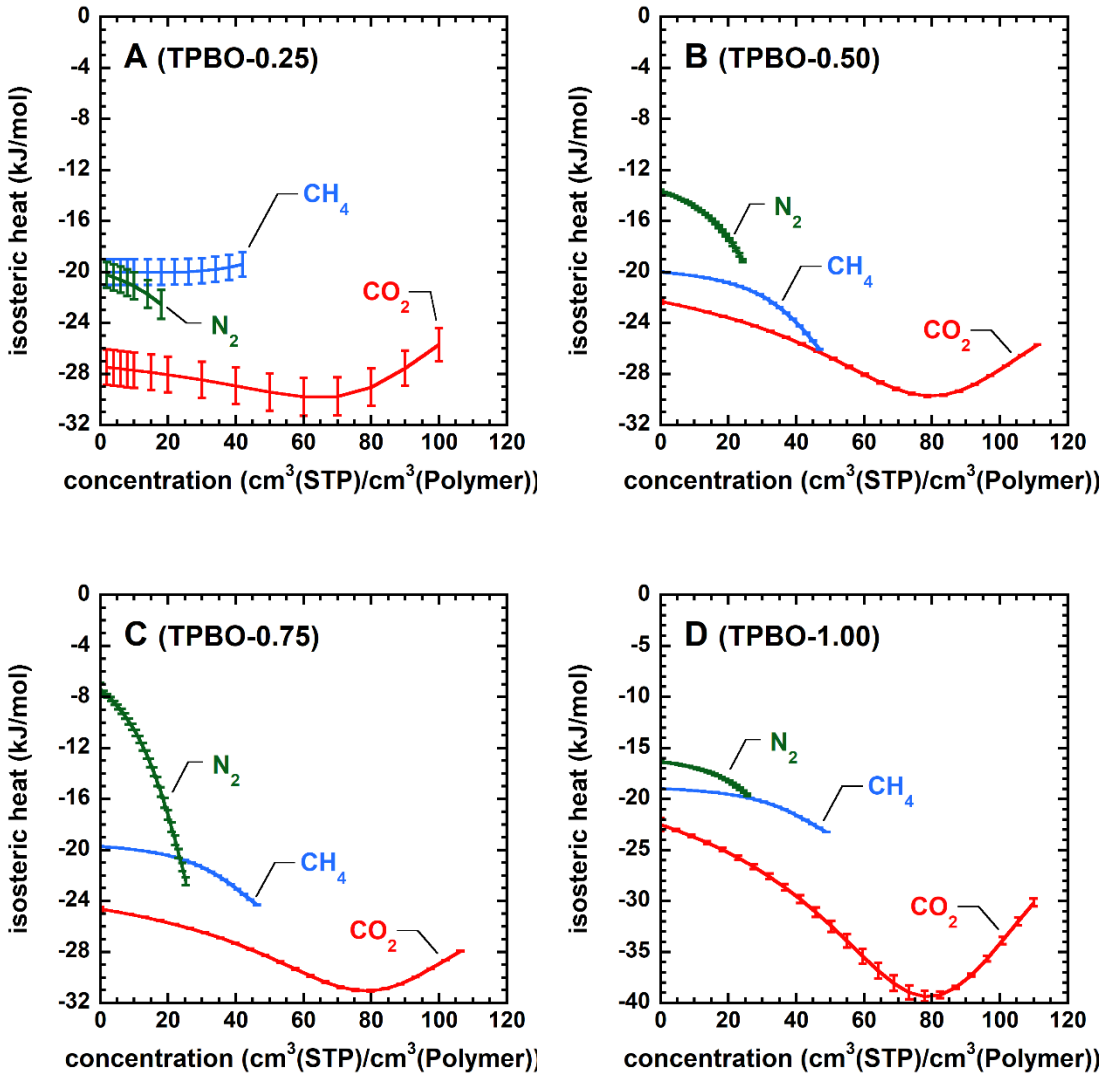

Figure 3. *Isosteric heat of N_2, CH_4 and CO_2 sorption in TPBO-0.25 (A), TPBO-0.50 (B), TPBO-0.75 (C) and TPBO-1.00 (D) as a function of penetrant concentration in the polymer. Error bars were estimated using the standard error of weighted linear regression [55]. Continuous lines are drawn to guide the eye.*

As noted in previous studies, taking into account the compressibility factor in Eq. 3 (i.e., Z, estimated using the Peng-Robinson equation of state) does not produce any relevant effect on the calculated isosteric heats, therefore Z was assumed equal to one [37, 43]. As expected, in all the TPBO samples and at any given concentration, sorption becomes more exothermic with

increasing penetrant condensability [59], that is, $\left|\Delta H_s^{CO_2}\right|$ (critical temperature = $304.19K$) > $\left|\Delta H_s^{CH_4}\right|$ (critical temperature = $190.8K$) > $\left|\Delta H_s^{N_2}\right|$ (critical temperature = $126.2K$) [60].

In all of the TPBO samples and within the experimental uncertainty, the isosteric heat of CH_4 and N_2 sorption slightly decreases or remains essentially constant with increasing penetrant concentration in the polymer. This behavior, which has been observed several times in glassy polymers, is consistent with the relatively low methane and nitrogen solubility in polymers, and their poor swelling ability [43]. In this condition, most of penetrant molecules are sorbed in the Langmuir's mode and, as long as more penetrant is sorbed in the matrix, the overall environment becomes more affine to penetrant molecules, which makes the sorption process more thermodynamically favorable (i.e., more exothermic) [37, 43]. In striking contrast, the isosteric heat of CO_2 sorption exhibits a well detectable minimum at the concentration of about 80 cm^3(STP)/cm^3(polymer) in all of the TPBO samples. At concentrations below 80 cm^3(STP)/cm^3(polymer), swelling is negligible as the vast majority of CO_2 molecules are sorbed in the Langmuir's mode. Above this concentration, sorption in the Henry's mode becomes significant and polymer swelling begins taking place [44]. This behavior is indicated by the sorption process becoming less exothermic at high CO_2 concentration, as the positive contribution of the deformation work needed to open transient gaps between polymer chains (i.e, ΔH_{mix}) partially overwhelms the largely negative contribution of the condensation enthalpy (i.e, ΔH_{cond}), according to the relationship [37, 43, 44]:

$$\Delta H_s = \Delta H_{cond} + \Delta H_{mix} \qquad \text{(Eq. 10)}$$

The fact that the position of the minimum is the same in all TPBO samples (i.e., ≅80 cm^3(STP)/cm^3(polymer)), is consistent with sorption being independent of triptycene content.

320 Moreover, this result indicates that triptycene units, while suppressing the membrane aging
321 propensity, do not help reduce swelling. In fact, if triptycene units were able to reduce swelling
322 and plasticization, the position of the minimum of isosteric heat of CO_2 sorption should
323 progressively shift to higher CO_2 concentration in TPBO samples containing higher molar amount
324 of triptycene units. Some recent permeability data in iptycene-containing polymers confirm this
325 picture, although a systematic study of plasticization and swelling in these materials is still
326 lacking [8].
327 Although the isosteric heat of sorption for any given penetrant is fairly independent of the
328 triptycene molar content (cf. Fig. S8, Supporting Information), the minimum in the isosteric heat
329 of CO_2 sorption becomes slightly more exothermic with increasing triptycene content. This result
330 might reflect an increased affinity between CO_2 molecules and the triptycene units. Moreover,
331 quadrupole interactions between polar CO_2 molecules and electron-rich triptycene clefts, as well
332 as the larger concentration of ether groups at higher molar triptycene content, may contribute to
333 this effect. Interestingly, these results are corroborated from the fact that while the isosteric heats
334 of N_2 and CH_4 sorption in TPBOs are similar, in absolute value, to the corresponding values
335 reported by Stevens et al. [56] in the case of polybenzoxazoles without triptycene groups, the
336 isosteric heat of CO_2 sorption in TPBOs is up to 40% larger than in triptycene-free
337 polybenzoxazoles. As mentioned above, however, this behavior could alternatively be ascribed
338 to the larger concentration of ether groups in TPBO samples exhibiting larger triptycene molar
339 content. Molecular simulations are underway to explain the fundamental origin of this behavior.
340

4.3 Pure- and mixed-gas solubility-selectivity. As shown in previous studies, the dual mode model provides a reliable prediction of mixed-gas sorption, as well as mixed-gas solubility-selectivity, using the three parameters, K_D, C'_H and b, retrieved from the analysis of experimental pure-gas sorption isotherms at the same temperature [61, 62]. Therefore, using Eqs. 7 and 9, mixed gas CO_2-CH_4 sorption isotherms in TPBOs from a 30%mol CO_2/70%mol CH_4 gas mixture were predicted at 35°C as a function of mixed-gas penetrant fugacity and compared to pure-gas sorption isotherms (cf., Fig.4). Mixed-gas CO_2 and CH_4 fugacity at 35°C and at the composition of interest was calculated, at multiple total pressures, with the Peng-Robinson equation of state, using a CO_2-CH_4 interaction parameter, k_{ij}, equal to 0.09 [63].

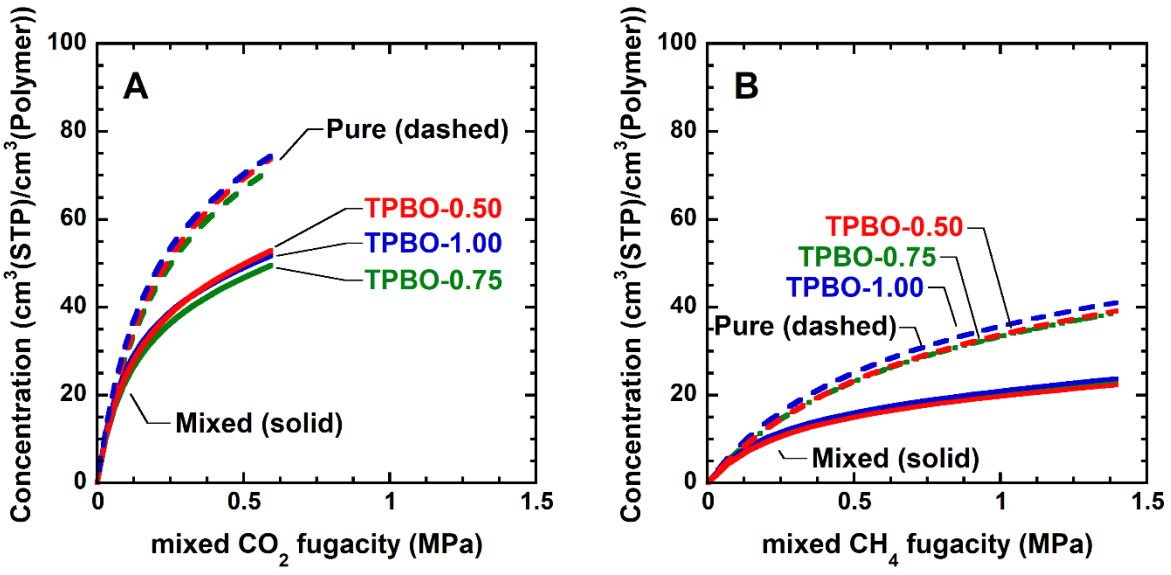

Figure 4. *Dual mode prediction of CO_2 (A) and CH_4 (B) mixed-gas isotherms from a 30% mol CO_2 / 70% mol CH_4 gas mixture in TPBOs as a function of mixed-gas fugacity at 35°C (solid lines), and comparison with pure gas sorption isotherms at the same temperature (dashed lines). Estimated uncertainty is shown in the Supporting Information (cf., Fig S9).*

As expected, in all TPBOs, sorption of the less condensable component (i.e., CH_4) in mixed-gas conditions is suppressed much more than that of the more condensable component (i.e., CO_2) relative to the pure gas conditions at the same temperature and fugacity. Specifically, at mixed gas fugacity of 0.6 MPa and 1.4 MPa for CO_2 and CH_4, respectively, sorption was reduced by 24-31% for CO_2 and 40-43% for CH_4 relative to pure gas at the same fugacity, with no substantial difference among TPBO samples, that is, irrespective of the triptycene molar content (cf. Fig. 4). Therefore, competitive sorption is essentially independent of triptycene content, indicating that configurational free volume has little or no effect on pure- and mixed-gas solubility and solubility-selectivity. To avoid any confusion and make the reading easier, error bars are not shown in Fig. 4. The uncertainty of predicted mixed-gas sorption data is provided in the Supporting Information (cf., Fig. S9-S10).

The results discussed above indicate that competitive sorption enhances mixed-gas CO_2/CH_4 solubility-selectivity relative to ideal solubility-selectivity. As shown in Fig. 5, for any TPBO sample, the predicted mixed-gas sorption-selectivity exceeds the experimental pure-gas sorption-selectivity by $18.3\% \pm 4\%$ at a CO_2 fugacity of 0.5 MPa. As discussed above, however, the increase in mixed-gas solubility-selectivity relative to ideal solubility-selectivity is fairly independent of polymer's triptycene molar content. To compare pure-gas and mixed-gas sorption selectivity on a more realistic basis, ideal (i.e, pure-gas) solubility-selectivity shown in Fig. 5 was calculated using pure-gas solubility data at the same fugacity as the mixed-gas case at any given pressure.

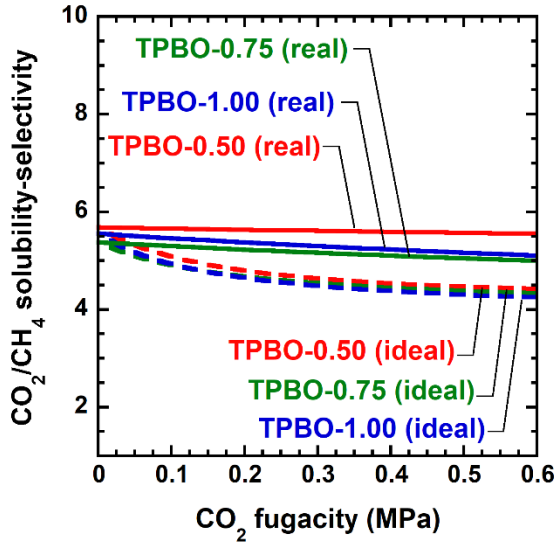

Figure 5. *Dual mode prediction of mixed-gas CO_2/CH_4 solubility-selectivity for a 30%mol CO_2 / 70% mol CH_4 mixture in TPBOs as a function of mixed-gas CO_2 fugacity at 35°C (solid line), and comparison with pure-gas CO_2/CH_4 solubility-selectivity (dashed line). Estimated uncertainty is shown in the Supporting Information (cf., Fig S10).*

Using the dual mode parameters estimated from the analysis of experimental pure-gas sorption isotherms, CO_2/CH_4 solubility-selectivity at CO_2 and CH_4 fugacity of 0.3 MPa and 0.7 MPa, respectively, is predicted to increase with decreasing temperatures (cf. Fig. S11, Supporting Information).

The most relevant result of this pure- and mixed-gas sorption study is that the incorporation of configurational free volume does not influence sorption and sorption-selectivity, therefore, according to the solution-diffusion model, diffusivity-selectivity is the only property affected by changes in triptycene content. This aspect will be discussed in section 4.4.

4.4 Mechanism of light gas transport through configurational free volume. Pure-gas CO_2 and CH_4 permeability data at 35°C collected by Luo et al. [25] and solubility data at 35°C from this study were used to estimate pure-gas diffusivity in TPBOs at 35°C up to 1 MPa. At given pressure, pure-gas permeability and diffusivity decrease with increasing triptycene molar content (cf., Fig. 6A-B). In contrast, pure-gas CO_2/CH_4 selectivity at 35°C and given pressure (i.e., 1MPa) increases with increasing triptycene content in TPBOs (cf., Fig. 6C). Since, as discussed in section 4.1, light gas solubility in TPBOs is essentially independent of triptycene molar content, we can conclude that, based on the solution-diffusion model, the permeability decrease and selectivity increase with increasing triptycene molar content are ascribed to a change in the diffusion behavior only, which means that incorporation of triptycene unity on the polymer backbone only influences the membrane size-sieving ability, with negligible or no effect on sorption and sorption-selectivity. This physical picture, however, is limited to light gasses. As shown in a previous study from this laboratory [39], when the penetrant kinetic diameter exceeds the size of the configurational free volume elements, i.e., for bulky vapor molecules, sorption becomes size-controlled, meaning that triptycene groups reduce the sorption of vapor molecules whose size exceeds their internal size. In Fig. 6A-B, experimental CO_2 pure-gas permeability [25] and diffusivity isotherms (calculated as $\frac{P}{S}$) at 35°C in TPBOs exhibiting increasing molar amount of triptycene units are shown as a function of pressure. At any given pressure, the decrease in gas permeability with increasing triptycene molar content mirrors the parallel decrease in diffusivity.

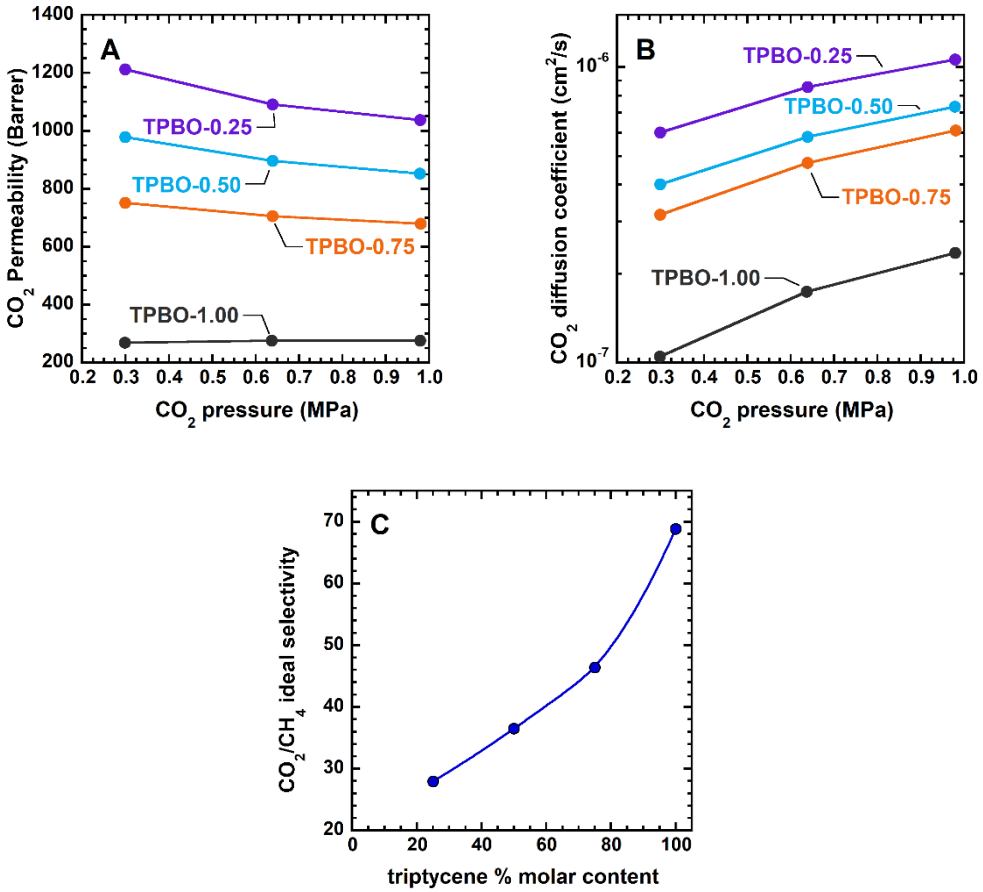

Figure 6. *Pure-gas CO_2 permeability (A) [25] and diffusivity (B) in TPBOs as a function of triptycene molar content and pressure at 35°C; pure-gas CO_2/CH_4 selectivity at 35°C and 1 MPa as a function of triptycene molar content (C). Similar results were obtained at other pressure values. Solid symbols are experimental data, and lines are drawn to guide the eye.*

As demonstrated below, this behavior is due to the strong size-sieving ability of triptycene units. To put these results in perspective, in Table 3 CO_2, CH_4 and N_2 permeability, diffusion coefficients and CO_2/CH_4 diffusivity-selectivity in TPBOs at 35°C and 1 MPa (i.e., 10 atm) are compared to benchmark polymers. Interestingly, TPBOs exhibit much larger diffusivity-selectivity compared to other polymers, which confirms that the size-sieving ability benefits much more than solubility-selectivity from configurational free volume.

Table 3. *Pure-gas permeability and diffusion coefficients, selectivity and diffusivity-selectivity in TPBOs and conventional polymer membrane materials at 35°C and 1 MPa (i.e., 10 atm).*

polymer	*permeability (Barrer)*			*diffusion coefficient (10^8 cm²/s)*			$\alpha_{\frac{CO_2}{CH_4}}$ *(ideal)*	$\alpha_{D,\frac{CO_2}{CH_4}}$ *(ideal)*
	CO_2	CH_4	N_2	CO_2	CH_4	N_2		
TPBO-0.25	*1042*	*37*	*57*	*125*	*9.3*	*37*	*28.2*	*13.4*
TPBO-0.50	*853*	*23*	*38*	*86*	*5.3*	*20*	*37.1*	*16.2*
TPBO-0.75	*680*	*15*	*27*	*69*	*3.3*	*14*	*45.3*	*20.9*
TPBO-1.00	*276*	*4.0*	*8.5*	*23*	*0.86*	*4.3*	*69.0*	*26.7*
PTMSP [64]	*21432*	*12192*	*5882*	*3300*	*3600*	*4300*	*1.75*	*0.9*
PDMS [65]	*3978*	*1200*	*380*	*2200*	*2200*	*3200*	3.3	1.0
PIM-1 [66]	*4419*	*388.5*	*288*	*360*	*73*	*130*	*11.4*	*4.9*
cellulose acetate [67]	*4.8*	*0.15*	/	*1.8*	*0.45*	/	*32.0*	*4*
Teflon® AF2400 [43]	*2332*	*383.4*	*475.7*	*678*	*290*	*600*	*6.1*	*2.3*
PEO [68]	*15.9*	*0.70*	*0.22*	*31*	*6.6*	*5.1*	*22.7*	*4.7*

Moreover, if the logarithm of permeability is plotted versus 1/FFV (cf. Fig. S12, Supporting Information), significant deviations from the expected linear trend are observed, which provides further evidence of the unique role played by configurational free volume in regulating small molecule transport in TPBOs.

To provide a more fundamental analysis of small molecule transport through configurational free volume-based polymers, the Henry's (i.e., D_D) and Langmuir's (i.e., D_H) mode contributions to CO_2 and CH_4 diffusion coefficients in TPBOs at 35°C were calculated using the dual-mode mobility model [50, 66]. To do so, for each penetrant and TPBO sample, permeability was plotted as a function of $\frac{C'_H b}{1+bf}$, to obtain a nice linear correlation, whose slope and intercept provide D_H and D_D, respectively. Details are provided in Fig. S13, Supporting Information. N_2 was excluded from this analysis, due to the larger uncertainty of permeability and solubility data relative to CH_4 and CO_2.

In Table 4, D_H and D_D values are compared among several glassy polymers of interest in gas separation. Uncertainties, calculated using the error propagation method, are shown in Figs. 7-A-B. Interestingly, while for any given penetrant in conventional glassy polymers D_D exceeds D_H by, at maximum, one order of magnitude, in TPBOs D_D exceeds D_H by at least two orders of magnitude [66], which highlights the superior size-sieving ability offered by triptycene units (i.e., configurational free volume).

Table 4. *Dual-mode mobility parameters for CO_2, CH_4, and N_2 in TPBOs, PIM-1, polysulfone (PSF), polycarbonate (PC) and 6FDA-6FpDA polyimide (PI). Data are at 35°C for all polymers except PIM-1, for which they are available at 25°C. Uncertainty of D_D and D_H values for TPBOs are shown in Figs. 7A-B.*

polymer	*gas*	*D_D (10^8 cm²/s)*	*D_H (10^8 cm²/s)*	*F*
TPBO-0.25	*CO_2*	*265.0*	*17.15*	*0.065*
	CH_4	*43.43*	*0.359*	*0.008*
TPBO-0.50	*CO_2*	*293.2*	*9.64*	*0.033*
	CH_4	*43.73*	*0.110*	*0.003*
TPBO-0.75	*CO_2*	*265.4*	*5.60*	*0.021*
	CH_4	*23.30*	*0.000*	*0.000*
TPBO-1.00	*CO_2*	*119.2*	*0.000*	*0.000*
	CH_4	*6.31*	*0.000*	*0.000*
PIM-1 [66]	*CO_2*	*1296.6*	*34.12*	*0.026*
	CH_4	*364*	*3.344*	*0.009*
PSF [69]	*CO_2*	*4.53*	*0.535*	*0.118*
	CH_4	*0.69*	*0.120*	*0.174*
PC [69]	*CO_2*	*6.22*	*0.485*	*0.078*
	CH_4	*1.09*	*0.125*	*0.115*
6FDA-6FpDA [70]	*CO_2*	*25.5*	*1.530*	*0.060*
	CH_4	*2.78*	*0.236*	*0.085*

Reporting D_H and D_D as a function of the molar triptycene content in TPBOs provides an opportunity to isolate and evaluate quantitatively the role of configurational free volume on light

gas transport. Interestingly, for both CO_2 and CH_4, the ratio D_H/D_D (referred to as F, cf. Eq. 6) in TPBOs systematically decreases with increasing the triptycene molar content, that is, with increasing the amount of configurational free volume (cf. Table 4). This result indicates that penetrant molecules trapped in the configurational free volume exhibit a very low mobility or no mobility at all as long as more triptycene units are incorporated in the polymer, which is consistent with the internal size of triptycene units being comparable to the penetrants size. This physical picture is further confirmed by the fact that the CO_2 and CH_4 Henry's (i.e., D_D) diffusion coefficients in TPBOs at 35°C are fairly constant, within the uncertainty, with increasing triptycene molar content, although a decrease is observed in the case of CH_4 in the TPBO-1.00 sample (cf., Fig. 7A-B) compared to the average of the other TPBO samples exhibiting lower triptycene molar content. This decrease, however, is not significant if we consider the uncertainty associated to D_D (cf. Fig. 7A-B). In contrast, the Langmuir's diffusion coefficient (i.e., D_H) decreases steadily with increasing triptycene molar amount. Interestingly, the decrease of CH_4 Langmuir's diffusivity with increasing triptycene content is steeper than the corresponding decrease of CO_2 Langmuir's diffusivity, which is consistent with CH_4 being a bulkier penetrant (kinetic diameter = 3.8Å) than CO_2 (kinetic diameter = 3.3Å) [71]. Therefore, the CH_4 size-exclusion becomes more effective with increasing amount of configurational free volume in the polymer. According to this physical picture, while $D_H^{CO_2}$ drops to zero (i.e. $F = 0$) in TPBO-1.00, $D_H^{CH_4}$ drops to zero already in TPBO-0.75, which, again, is consistent with CH_4 being a larger molecule than CO_2.

Different approaches have been used to estimate the size of the internal free volume of triptycene units. For example, PALS (Positron Annihilation Lifetime Spectroscopy) measurements suggest that the average free volume size is about 7Å [25]. However, due to the nature of PALS

measurements, this number provides the average size of all the free volume elements, including conformational and configurational free volume elements. Molecular simulations provide, for a single triptycene unit, an internal size less than 4 Å [26]. Finally, if we consider the space between two arene blades of triptycene units as a prism whose internal volume has been estimated to be 31 $Å^3$, the diameter of the corresponding sphere would be about 3.9 Å [26]. All these considerations indicate that the internal size of triptycene units is comparable to that of CH_4 molecules (kinetic diameter = 3.8Å), therefore triptycene units exclude CH_4 much more efficiently than CO_2 (kinetic diameter = 3.3Å), which supports the fact that $D_H^{CH_4}$ decreases faster than $D_H^{CO_2}$ with increasing molar amount of triptycene units in the polymer backbone.

The most relevant conclusion of this transport study is that penetrant ability to move within Langmuir sites of TPBOs is severely inhibited as the amount of triptycene increases. This result unequivocally demonstrates that the high size-sieving ability of TPBOs is essentially ascribed to configurational free volume, whose size is well-defined, stable and comparable to the size of one single molecule. In sharp contrast, the size of conformational free volume pockets generated by inefficient chain packing is randomly distributed and unstable over long-term operation [25, 33]. To provide a more quantitative evaluation of the enhanced size-sieving ability provided by configurational free volume, the Henry's (i.e., $D_D^{CO_2}/D_D^{CH_4}$) and Langmuir's (i.e., $D_H^{CO_2}/D_H^{CH_4}$) contributions to pure-gas CO_2/CH_4 diffusivity-selectivity have been estimated (cf. Fig. 7C). Although Henry's mode CO_2/CH_4 ideal diffusivity-selectivity at 35°C is essentially constant, within the experimental uncertainty, with increasing triptycene molar contents from 25 to 100%, the Langmuir's mode diffusivity-selectivity ranges from 48 in TPBO-0.25 to 88 in TPBO-0.50, and it becomes practically infinite in TPBO-0.75 and TPBO-1.00. This result further supports the idea

that triptycene units can finely regulate small molecule transport based on their size, indicating that the superior TPBOs' size-sieving ability is due primarily to configurational free volume, with other possible effects being negligible or at least less relevant.

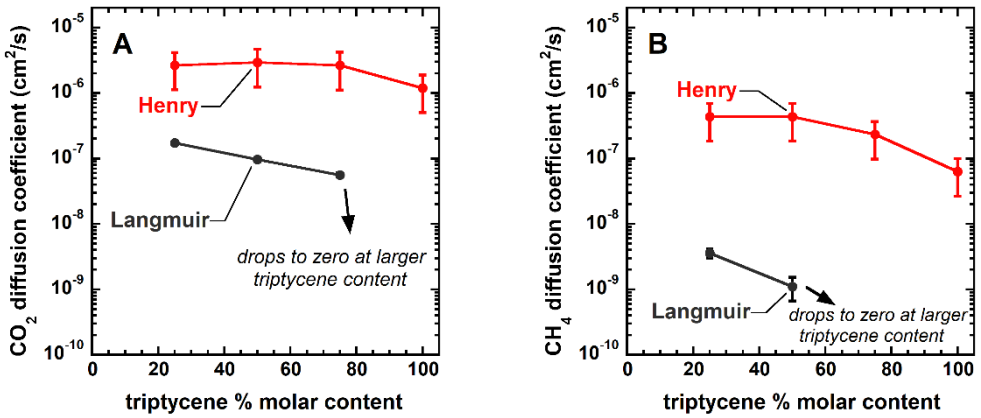

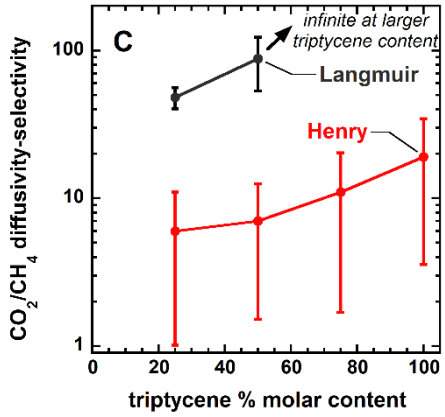

Figure 7. *Henry's and Langmuir's mode CO_2 (A) and CH_4 (B) diffusion coefficients, as well as CO_2/CH_4 Henry's (i.e., $D_D^{CO_2}/D_D^{CH_4}$) and Langmuir's (i.e., $D_H^{CO_2}/D_H^{CH_4}$) diffusivity-selectivity (C) in TPBOs at 35 °C as a function of triptycene molar content. $D_H^{CO_2}$ drops to zero in TPBO-1.00. $D_H^{CH_4}$ drops to zero when the triptycene molar content in the polymer is equal to 75% mol or larger. The Langmuir's diffusivity-selectivity, $D_H^{CO_2}/D_H^{CH_4}$, approaches infinite when the triptycene molar content is equal to 75% mol or larger. Uncertainty was calculated using linear error propagation [55].*

5. Conclusions

A class of polybenzoxazoles (TPBOs) with systematically varied molar amount of triptycene units (i.e., configurational free volume) was selected to propose a possible mechanism of small molecule transport in glassy polymers exhibiting configurational free volume. At given temperature and pressure, pure-gas permeability decreases and ideal selectivity increases with increasing triptycene molar content in TPBOs. The analysis of pure-gas N_2, CH_4 and CO_2 sorption isotherms indicates that gas solubility and solubility-selectivity are essentially independent of triptycene molar content. Similarly, mixed-gas CO_2/CH_4 sorption isotherms predicted using the dual mode model show that competitive sorption (i.e., mixed-gas solubility-selectivity) is independent of triptycene molar content. Therefore, the decrease in gas permeability with increasing triptycene content in TPBOs mirrors the parallel decrease in diffusion coefficient, and the increase in selectivity with increasing molar amount of triptycene units mirrors the parallel increase in diffusivity-selectivity (i.e., size-sieving ability).

The dual mode sorption-mobility analysis indicates that small molecule diffusion in TPBOs is progressively hindered with increasing triptycene molar content (that is, with increasing configurational free volume), with a stronger hinderance offered to the transport of larger molecules. Interestingly, while the Henry's CO_2/CH_4 diffusivity-selectivity (i.e., $D_D^{CO_2}/D_D^{CH_4}$) changes little with increasing triptycene molar content, the Langmuir's CO_2/CH_4 diffusivity-selectivity (i.e., $D_H^{CO_2}/D_H^{CH_4}$) rapidly increases with increasing amount of configurational free volume, to become infinite when the molar amount of triptycene units in the polymer is equal to 75% or larger. Therefore, configurational free volume provides a unique opportunity to precisely control diffusivity-selectivity in a predictable fashion. Equally important, in contrast with

conformational free volume, configurational free volume exhibits excellent resistance to physical aging, which makes configurational diffusivity-selectivity highly stable over long-term operation. This physical picture, however, is limited to light gasses. As shown in a previous study [39], when the penetrant kinetic diameter exceeds the size of the configurational free volume elements, sorption becomes size-controlled, meaning that triptycene units influence both sorption and diffusion coefficients.

Finally, the analysis of isosteric heats of sorption reveals that the TPBOs plasticization resistance does not increase with increasing triptycene molar content. Ongoing and future work will investigate the effect of configurational free volume content on the simultaneous transport of gas (i.e., small) and vapor (i.e., bulky) molecules.

Acknowledgements

Financial support from the US National Science Foundation (NSF) under the grant CBET-1926868 (*Interfacial Engineering*) is gratefully acknowledged. ZH and RG also acknowledge partial support from the National Science Foundation under Cooperative Agreement No. EEC-1647722.

References

[1] J. Deng, Z. Huang, B.J. Sundell, D.J. Harrigan, S.A. Sharber, K. Zhang, R. Guo, M. Galizia, State of the art and prospects of chemically and thermally aggressive membrane gas separations: Insights from polymer science, Polymer, 229 (2021) 123988.
[2] M. Galizia, W.S. Chi, Z.P. Smith, T.C. Merkel, R.W. Baker, B.D. Freeman, 50th anniversary perspective: polymers and mixed matrix membranes for gas and vapor separation: a review and prospective opportunities, Macromolecules, 50 (2017) 7809-7843.
[3] L.M. Robeson, Correlation of separation factor versus permeability for polymeric membranes, J. Membr. Sci., 62 (1991) 165-185.
[4] L.M. Robeson, The upper bound revisited, J. Membr. Sci., 320 (2008) 390-400.

[5] J.R. Weidman, R. Guo, The use of iptycenes in rational macromolecular design for gas separation membrane applications, Ind. Eng. Chem. Res., 56 (2017) 4220-4236.
[6] P.M. Budd, B.S. Ghanem, S. Makhseed, N.B. McKeown, K.J. Msayib, C.E. Tattershall, Polymers of intrinsic microporosity (PIMs): robust, solution-processable, organic nanoporous materials, Chemical communications, (2004) 230-231.
[7] P.M. Budd, N.B. McKeown, D. Fritsch, Polymers of intrinsic microporosity (PIMs): high free volume polymers for membrane applications, in: Macromolecular Symposia, Wiley Online Library, New York, 2006, pp. 403-405.
[8] T.J. Corrado, Z. Huang, D. Huang, N. Wamble, T. Luo, R. Guo, Pentiptycene-based ladder polymers with configurational free volume for enhanced gas separation performance and physical aging resistance, Proceedings of the National Academy of Sciences, 118 (2021).
[9] H.B. Park, C.H. Jung, Y.M. Lee, A.J. Hill, S.J. Pas, S.T. Mudie, E. Van Wagner, B.D. Freeman, D.J. Cookson, Polymers with cavities tuned for fast selective transport of small molecules and ions, Science, 318 (2007) 254-258.
[10] C.H. Lau, P.T. Nguyen, M.R. Hill, A.W. Thornton, K. Konstas, C.M. Doherty, R.J. Mulder, L. Bourgeois, A.C. Liu, D.J. Sprouster, Ending aging in super glassy polymer membranes, Angewandte Chemie International Edition, 53 (2014) 5322-5326.
[11] H. Lin, E. Van Wagner, B.D. Freeman, L.G. Toy, R.P. Gupta, Plasticization-enhanced hydrogen purification using polymeric membranes, Science, 311 (2006) 639-642.
[12] T.C. Merkel, I. Pinnau, R. Prabhakar, B.D. Freeman, Gas and vapor transport properties of perfluoropolymers, Materials science of membranes for gas and vapor separation, 1 (2006) 251.
[13] M. Yavari, M. Fang, H. Nguyen, T.C. Merkel, H. Lin, Y. Okamoto, Dioxolane-based perfluoropolymers with superior membrane gas separation properties, Macromolecules, 51 (2018) 2489-2497.
[14] Y. Okamoto, H.-C. Chiang, M. Fang, M. Galizia, T. Merkel, M. Yavari, H. Nguyen, H. Lin, Perfluorodioxolane polymers for gas separation membrane applications, Membranes, 10 (2020) 394.
[15] B.D. Freeman, Basis of permeability/selectivity tradeoff relations in polymeric gas separation membranes, Macromolecules, 32 (1999) 375-380.
[16] Z. Ali, B.S. Ghanem, Y. Wang, F. Pacheco, W. Ogieglo, H. Vovusha, G. Genduso, U. Schwingenschlögl, Y. Han, I. Pinnau, Finely tuned submicroporous thin-film molecular sieve membranes for highly efficient fluid separations, Adv. Mater., 32 (2020) 2001132.
[17] A.M. Tandel, W. Guo, K. Bye, L. Huang, M. Galizia, H. Lin, Designing organic solvent separation membranes: polymers, porous structures, 2D materials, and their combinations, Materials Advances, 2 (2021) 4574-4603.
[18] G.M. Geise, H.B. Park, A.C. Sagle, B.D. Freeman, J.E. McGrath, Water permeability and water/salt selectivity tradeoff in polymers for desalination, J. Membr. Sci., 369 (2011) 130-138.
[19] P. Marchetti, M.F. Jimenez Solomon, G. Szekely, A.G. Livingston, Molecular separation with organic solvent nanofiltration: a critical review, Chem. Rev., 114 (2014) 10735-10806.
[20] Y. Yampolskii, N. Belov, A. Alentiev, Perfluorinated polymers as materials of membranes for gas and vapor separation, J. Membr. Sci., 598 (2020) 117779.
[21] B. Comesaña-Gándara, J. Chen, C.G. Bezzu, M. Carta, I. Rose, M.-C. Ferrari, E. Esposito, A. Fuoco, J.C. Jansen, N.B. McKeown, Redefining the Robeson upper bounds for CO_2/CH_4 and

598 CO_2/N_2 separations using a series of ultrapermeable benzotriptycene-based polymers of intrinsic
599 microporosity, Energy & Environmental Science, 12 (2019) 2733-2740.
600 [22] Y.J. Cho, H.B. Park, Gas separation properties of triptycene-based polyimide membranes, in:
601 I. Escobar, B. Van der Bruggen (Eds.), Modern Applications in Membrane Science and
602 Technology, ACS Publications, Washington DC, 2011, pp. 107-128.
603 [23] T. Corrado, Z. Huang, J. Aboki, R. Guo, Microporous polysulfones with enhanced separation
604 performance via integration of the triptycene moiety, Ind. Eng. Chem. Res., 59 (2019) 5351-5361.
605 [24] S. Luo, J.R. Wiegand, P. Gao, C.M. Doherty, A.J. Hill, R. Guo, Molecular origins of fast and
606 selective gas transport in pentiptycene-containing polyimide membranes and their physical
607 aging behavior, J. Membr. Sci., 518 (2016) 100-109.
608 [25] S. Luo, Q. Zhang, L. Zhu, H. Lin, B.A. Kazanowska, C.M. Doherty, A.J. Hill, P. Gao, R. Guo,
609 Highly selective and permeable microporous polymer membranes for hydrogen purification and
610 CO2 removal from natural gas, Chem. Mater., 30 (2018) 5322-5332.
611 [26] J.R. Weidman, S. Luo, C.M. Doherty, A.J. Hill, P. Gao, R. Guo, Analysis of governing factors
612 controlling gas transport through fresh and aged triptycene-based polyimide films, J. Membr.
613 Sci., 522 (2017) 12-22.
614 [27] L. Zhao, Z. Li, T. Wirth, Triptycene derivatives: synthesis and applications, Chem. Lett., 39
615 (2010) 658-667.
616 [28] Y. Jiang, C.F. Chen, Recent developments in synthesis and applications of triptycene and
617 pentiptycene derivatives, European Journal of Organic Chemistry, 2011 (2011) 6377-6403.
618 [29] Y. Jiang, F.T. Willmore, D. Sanders, Z.P. Smith, C.P. Ribeiro, C.M. Doherty, A. Thornton, A.J.
619 Hill, B.D. Freeman, I.C. Sanchez, Cavity size, sorption and transport characteristics of thermally
620 rearranged (TR) polymers, Polymer, 52 (2011) 2244-2254.
621 [30] S. Luo, J.R. Wiegand, B. Kazanowska, C.M. Doherty, K. Konstas, A.J. Hill, R. Guo, Finely
622 tuning the free volume architecture in iptycene-containing polyimides for highly selective and
623 fast hydrogen transport, Macromolecules, 49 (2016) 3395-3405.
624 [31] J.R. Wiegand, Z.P. Smith, Q. Liu, C.T. Patterson, B.D. Freeman, R. Guo, Synthesis and
625 characterization of triptycene-based polyimides with tunable high fractional free volume for gas
626 separation membranes, Journal of Materials Chemistry A, 2 (2014) 13309-13320.
627 [32] R.D. Crist, Z. Huang, R. Guo, M. Galizia, Effect of thermal treatment on the structure and gas
628 transport properties of a triptycene-based polybenzoxazole exhibiting configurational free
629 volume, J. Membr. Sci., 597 (2020) 117759.
630 [33] Y. Huang, D.R. Paul, Physical aging of thin glassy polymer films monitored by gas
631 permeability, Polymer, 45 (2004) 8377-8393.
632 [34] M.M. Merrick, R. Sujanani, B.D. Freeman, Glassy polymers: Historical findings, membrane
633 applications, and unresolved questions regarding physical aging, Polymer, 211 (2020) 123176.
634 [35] S.J. Smith, R. Hou, K. Konstas, A. Akram, C.H. Lau, M.R. Hill, Control of physical aging in
635 super-glassy polymer mixed matrix membranes, Acc. Chem. Res., 53 (2020) 1381-1388.
636 [36] Z.-X. Low, P.M. Budd, N.B. McKeown, D.A. Patterson, Gas permeation properties, physical
637 aging, and its mitigation in high free volume glassy polymers, Chem. Rev., 118 (2018) 5871-5911.
638 [37] V. Loianno, S. Luo, Q. Zhang, R. Guo, M. Galizia, Gas and water vapor sorption and diffusion
639 in a triptycene-based polybenzoxazole: effect of temperature and pressure and predicting of
640 mixed gas sorption, J. Membr. Sci., 574 (2019) 100-111.

[38] V. Loianno, Q. Zhang, S. Luo, R. Guo, M. Galizia, Modeling gas and vapor sorption and swelling in triptycene-based polybenzoxazole: Evidence for entropy-driven sorption behavior, Macromolecules, 52 (2019) 4385-4395.
[39] W.J. Box, Z. Huang, R. Guo, M. Galizia, Evidence for Size-Sieving Driven Vapor Sorption and Diffusion in a Glassy Polybenzoxazole Exhibiting Configurational Free Volume, Ind. Eng. Chem. Res., 60 (2021) 13326-13337.
[40] J.G. Wijmans, R.W. Baker, The solution-diffusion model: a review, J. Membr. Sci., 107 (1995) 1-21.
[41] K.P. Bye, V. Loianno, T.N. Pham, R. Liu, J.S. Riffle, M. Galizia, Pure and mixed fluid sorption and transport in Celazole® polybenzimidazole: Effect of plasticization, J. Membr. Sci., 580 (2019) 235-247.
[42] W. Koros, D. Paul, G. Huvard, Energetics of gas sorption in glassy polymers, Polymer, 20 (1979) 956-960.
[43] T. Merkel, V. Bondar, K. Nagai, B. Freeman, Y.P. Yampolskii, Gas sorption, diffusion, and permeation in poly (2, 2-bis (trifluoromethyl)-4, 5-difluoro-1, 3-dioxole-co-tetrafluoroethylene), Macromolecules, 32 (1999) 8427-8440.
[44] V. Loianno, K.P. Bye, M. Galizia, P. Musto, Plasticization mechanism in polybenzimidazole membranes for organic solvent nanofiltration: Molecular insights from in situ FTIR spectroscopy, J. Polym. Sci., 58 (2020) 2547-2560.
[45] M. Omidvar, H. Nguyen, J. Liu, H. Lin, Sorption-enhanced membrane materials for gas separation: a road less traveled, Current Opinion in Chemical Engineering, 20 (2018) 50-59.
[46] R. Felder, C. Patton, W. Koros, Dual-mode sorption and transport of sulfur dioxide in kapton polyimide, J. Polym. Sci.: Polym. Phys. Ed., 19 (1981) 1895-1909.
[47] R. Barrer, Diffusivities in glassy polymers for the dual mode sorption model, J. Membr. Sci., 18 (1984) 25-35.
[48] R. Chern, W. Koros, E. Sanders, S. Chen, H. Hopfenberg, Implications of the dual-mode sorption and transport models for mixed gas permeation, in, ACS Publications, 1983.
[49] J. Petropoulos, On the dual mode gas transport model for glassy polymers, J. Polym. Sci. B: Polymer Physics, 26 (1988) 1009-1020.
[50] D. Paul, W. Koros, Effect of partially immobilizing sorption on permeability and the diffusion time lag, J. Polym. Sci.: Polym. Phys. Ed., 14 (1976) 675-685.
[51] W. Koros, Model for sorption of mixed gases in glassy polymers, J. Polym. Sci.: Polym. Phys. Ed., 18 (1980) 981-992.
[52] Q. Liu, M. Galizia, K.L. Gleason, C.A. Scholes, D.R. Paul, B.D. Freeman, Influence of toluene on CO2 and CH4 gas transport properties in thermally rearranged (TR) polymers based on 3, 3′-dihydroxy-4, 4′-diamino-biphenyl (HAB) and 2, 2′-bis-(3, 4-dicarboxyphenyl) hexafluoropropane dianhydride (6FDA), J. Membr. Sci., 514 (2016) 282-293.
[53] D.W. Van Krevelen, K. Te Nijenhuis, Properties of polymers: their correlation with chemical structure; their numerical estimation and prediction from additive group contributions, Elsevier, Amsterdam, 2009.
[54] D.-Y. Peng, D.B. Robinson, A new two-constant equation of state, Ind. Eng. Chem. Fund., 15 (1976) 59-64.

[55] P.R. Bevington, D.K. Robinson, Data reduction and error analysis, McGraw-Hill, New York, (2003).
[56] K.A. Stevens, Z.P. Smith, K.L. Gleason, M. Galizia, D.R. Paul, B.D. Freeman, Influence of temperature on gas solubility in thermally rearranged (TR) polymers, J. Membr. Sci., 533 (2017) 75-83.
[57] W. Koros, D. Paul, CO_2 sorption in poly (ethylene terephthalate) above and below the glass transition, J. Polym. Sci.: Polym. Phys. Ed., 16 (1978) 1947-1963.
[58] R.S. Prabhakar, B.D. Freeman, I. Roman, Gas and vapor sorption and permeation in poly (2, 2, 4-trifluoro-5-trifluoromethoxy-1, 3-dioxole-co-tetrafluoroethylene), Macromolecules, 37 (2004) 7688-7697.
[59] F. Körösy, Two rules concerning solubility of gases and crude data on solubility of krypton, Transactions of the Faraday Society, 33 (1937) 416-425.
[60] R.C. Reid, J.M. Prausnitz, B.E. Poling, The properties of gases and liquids, (1987).
[61] E. Sanders, W. Koros, H. Hopfenberg, V. Stannett, Mixed gas sorption in glassy polymers: Equipment design considerations and preliminary results, J. Membr. Sci., 13 (1983) 161-174.
[62] E. Sanders, W.J. Koros, H. Hopfenberg, V. Stannett, Pure and mixed gas sorption of carbon dioxide and ethylene in poly (methyl methacrylate), J. Membr. Sci., 18 (1984) 53-74.
[63] S.I. Sandler, Chemical, biochemical, and engineering thermodynamics, John Wiley & Sons, 2017.
[64] T. Merkel, V. Bondar, K. Nagai, B. Freeman, Sorption and transport of hydrocarbon and perfluorocarbon gases in poly (1-trimethylsilyl-1-propyne), Journal of Polymer Science Part B: Polymer Physics, 38 (2000) 273-296.
[65] T. Merkel, V. Bondar, K. Nagai, B. Freeman, I. Pinnau, Gas sorption, diffusion, and permeation in poly (dimethylsiloxane), J. Polym. Sci. B: Polymer Physics, 38 (2000) 415-434.
[66] P. Li, T.-S. Chung, D. Paul, Gas sorption and permeation in PIM-1, J. Membr. Sci., 432 (2013) 50-57.
[67] A. Houde, B. Krishnakumar, S. Charati, S. Stern, Permeability of dense (homogeneous) cellulose acetate membranes to methane, carbon dioxide, and their mixtures at elevated pressures, J. Appl. Polym. Sci., 62 (1996) 2181-2192.
[68] H. Lin, B.D. Freeman, Gas solubility, diffusivity and permeability in poly (ethylene oxide), J. Membr. Sci., 239 (2004) 105-117.
[69] T. Barbari, W. Koros, D. Paul, Gas transport in polymers based on bisphenol-A, J. Polym. Sci. B: Polymer Physics, 26 (1988) 709-727.
[70] R. Wang, C. Cao, T.-S. Chung, A critical review on diffusivity and the characterization of diffusivity of 6FDA–6FpDA polyimide membranes for gas separation, J. Membr. Sci., 198 (2002) 259-271.
[71] L.M. Robeson, M.E. Dose, B.D. Freeman, D.R. Paul, Analysis of the transport properties of thermally rearranged (TR) polymers and polymers of intrinsic microporosity (PIM) relative to upper bound performance, J. Membr. Sci., 525 (2017) 18-24.